THE JOURNAL OF PHYSICAL CHEMISTRY B

Article

pubs.acs.org/JPCB

Aqueous Solvation of Methane from First Principles

Lorenzo Rossato, Francesco Rossetto, and Pier Luigi Silvestrelli*

Dipartimento di Fisica e Astronomia "G. Galilei", Università di Padova, via Marzolo 8, I-35131 Padova, Italy, and DEMOCRITOS National Simulation Center, Trieste, Italy

ABSTRACT: Structural, dynamical, bonding, and electronic properties of water molecules around a soluted methane molecule are studied from first principles. The results are compatible with experiments and qualitatively support the conclusions of recent classical molecular dynamics simulations concerning the controversial issue on the presence of "immobilized" water molecules around hydrophobic groups: the hydrophobic solute slightly reduces (by a less than 2 factor) the mobility of many surrounding water molecules rather than immobilizing just the few ones which are closest to methane, similarly to what was obtained by previous first-principles simulations of soluted methanol. Moreover, the rotational slowing down is compatible with the one predicted on the basis of the excluded volume fraction, which leads to a slower hydrogen bond exchange rate. The analysis of simulations performed at different temperatures suggests that the target temperature of the soluted system must be carefully chosen, in order to avoid artificial slowing-down effects. By generating maximally localized Wannier functions, a detailed description of the polarization effects in both solute and solvent molecules is obtained, which better characterizes the solvation process.

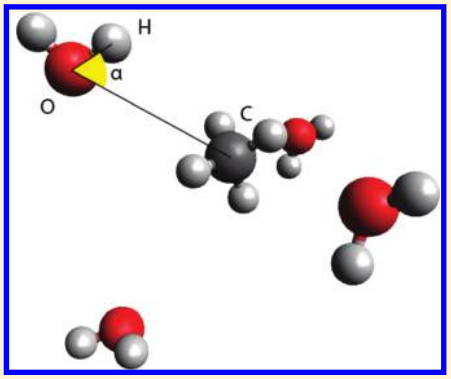

I. INTRODUCTION

Understanding the properties of water around hydrophobic solutes, which are mainly determined by the hydrogen bond (Hb) network, is crucial, since the rotational and translational motion of water molecules in solution control the rates of important chemical and biochemical processes,[1,2] such as protein folding and membrane assembly. Basically, the hydrophobic effect represents the tendency of apolar groups to associate in aqueous solutions and minimize the total surface that is exposed to water; instead, polar groups can participate in Hb's with water molecules.

In particular, the aqueous solution properties of methane have long been of interest: in fact, methane is the simplest hydrocarbon molecule and represents a good model compound for understanding the properties of water molecules in the solvation shell of small apolar solutes. Methane−water systems also play an important role in various fields of the natural sciences, ranging from fossil fuel chemistry to reactions in the conversion of solar energy (thermochemistry) to methane production from fermentation of farm wastes.[3]

It is now generally believed that the nature of hydrophobicity is size dependent:[4] small apolar molecules such as methane have a hydration free energy near ambient conditions that is largely entropic; that is, it depends more on the number of ways all of the water molecules in the methane hydration shell can form Hb's rather than their energies. Water molecules in the vicinity of small nonpolar solutes are capable[5] of rearranging themselves in such a way to encapsulate the guest molecule and to regenerate any Hb's broken during the insertion of the solute, so that a nonpolar solute can be thought of as a "structure maker";[5,6] it is then possible to describe hydrophobic hydration in terms of the directional, hydrogen bonding properties of water, which undergoes a restricted orientational freedom due to the inability of the solute to participate in Hb's, which makes certain orientations of the hydration shell water molecules energetically unfavorable.[5]

In spite of the importance of the subject, a detailed, microscopic understanding of water dynamics in the vicinity to an apolar solute remains elusive and different mechanisms have been conjectured. It was suggested[7] that hydrophobic solutes enforce the network of H-bonded water molecules around them and strongly decrease their mobility, in such a way that they form rigid, icelike structures ("icebergs"). However, several experimental and computational studies showed that, at least at low solute concentration around room temperature, the structure and dynamics of the water molecules in the solvation shell is similar to that of bulk water.[8−12] Nuclear magnetic resonance (NMR) and dielectric relaxation (DR) experiments[13] indicated that the mobility of water molecules in solutions containing hydrophobic solutes is decreased; however, since these methods can only measure a response averaged over all water molecules, it was not clear whether well-defined layers of "immobilized" water molecules exist or instead there are many molecules slightly affected in their dynamical behavior. Recent results by Rezus and Bakker,[2] obtained by using femtosecond mid-infrared spectroscopy (fs-IR) to investigate the hydration of hydrophobic groups on a subpicosecond time scale (experiments[14] use "ultrashort"-infrared pulses with durations of the order of 50 fs), have been interpreted as a confirmation that water molecules surrounding hydrophobic groups undergo

Received: January 24, 2012
Revised: March 20, 2012
Published: March 23, 2012

a much slower orientational dynamics than the bulk liquid and are therefore effectively immobilized; in particular, it is suggested that each methyl group is surrounded by four immobilized waters, supporting the "iceberg" picture in a *dynamical* way: although the water molecules around hydrophobic groups have liquidlike structures, their dynamics would be icelike, which also explains why hydrophobic icebergs were not previously observed with structural methods.

The major experimental problem in the NMR measurements of water−methane systems is due to the low solubility of methane in water; in readily accessible proton spectra, a large proton water peak would effectively mask the signal from small amounts of dissolved methane.[3] Computer simulations can give very detailed information about the solvation structure, providing detailed mechanistic insights that cannot be directly obtained from experiments. In one of the first classical molecular dynamics (MD) simulations of methane−water systems, Laaksonen and Stilbs[3] found that the dynamics of the solvent water molecules is slowed down (by about a 1.5 factor in the reorientational correlation time): in particular, the reorientational motion is sensitive to the presence of methane in solution; the simulated translational diffusion of methanes as solutes is also slowed down but is higher than observed experimentally. Moreover, methane acts nearly as a free rotor.[3]

Subsequent classical MD simulations[9−12] supported the idea that a moderate slowing down of water dynamics around hydrophobic groups arises from a steric effect, with a consequent decrease in the configurational space available to water molecules around hydrophobic solutes. Interestingly, Stirnemann et al.[15] investigated the Hb dynamics of water in a series of amphiphilic solute solutions (solute molecules possessing both hydrophobic and hydrophilic moieties) through classical MD simulations and analytic modeling: they find that for most solutes the major effect in the hydration dynamics comes from the hydrophilic groups that can retard the water dynamics much more significantly (the retardation factor being about 1.4) than can hydrophobic groups by forming strong Hb's with water; by contrast, hydrophobic groups are shown to have a very moderate effect on water Hb breaking kinetics via an excluded volume effect.[15] This interpretation is in contrast with, for instance, that of Bakulin et al.[16] who studied solvation of tetramethylurea and other amphiphilic solutes, and attribute the retarded spectral relaxation observed in the experimental spectra to a dramatic slowdown in the water dynamics induced by the hydrophobic groups, due to the suppression of water jumps between Hb acceptors: in particular, due to a steric effect, the fifth water molecule which is required to form a defect state in the tetrahedral surroundings (with the temporary formation of a bifurcated Hb) cannot approach the H-bonded pair to initiate the molecular jump; as a result, the rate of the jumping events sharply decreases, which, in turn, strongly slows the rotation of the water molecules.[16] Therefore, the effect of hydrophobic groups would be twofold: they do not only exclude part of the volume available for switching but fundamentally change the Hb dynamics of the solvating water molecules; this can be associated with the formation of a more "rigid" water−solute structure where the translational mobility decreases; this explanation is supported by the suppressed translational mobility of water and its excellent correlation to Hb dynamics.[16] Bakulin et al.[16] interpret their results as a demonstration that the hydrophilic part of the molecules does not play an important role in the water Hb dynamics. Note, however, that the strong slowing down of the reorientation in the hydrophobic hydration shells is not reproduced by MD simulations:[9,17] for instance, in a classical MD study (using SPC/E water), the reorientation of OH groups tangential to hydrophobic methyl groups was calculated to slow down only by a factor of about 1.4 at low solute concentrations.[9] On the basis of these observations and controversial interpretations, it appears to be extremely useful to perform accurate first principles simulations to study a system where hydrophilic groups are absent in such a way to investigate the effect of a hydrophobic group only. In fact, MD simulations based on empirical force fields, specifically designed to reproduce selected experimental data or a limited set of quantum chemically computed structures, do not provide a description completely independent from reference data and the reliability of the results, at conditions significantly different from those where the potential was designed for, may be questionable. These limitations can be overcome by Car−Parrinello MD simulations, where the interactions are calculated from first principles, and that have been already used in studies of liquid water,[18−22] aqueous solvation,[17,23−27] and nucleic acid models containing both hydrophilic and hydrophobic groups.[28,29] With respect to force-field-based MD, first principles MD has important advantages: it naturally incorporates polarization, it accounts for the intramolecular motion, and it gives detailed information on the electronic properties such as the charge distribution.

We have recently studied[17] the interaction of water with methanol (the simplest alcohol), which can be considered as a prototype of a solute with both hydrophobic (methyl) and hydrophilic (hydroxyl) groups: we found that the presence of a methanol molecule slightly reduces the mobility of many water molecules, rather than immobilizing just the few ones which are closest to the methyl group, in line with the interpretation of Qvist and Halle[12] and with classical MD simulation results.[9,30] Here we study, from first principles, the interaction of water with methane which can be considered as a prototype of an hydrophobic solute. A previous first principles study of a water−methane solution exists, which was however limited to the investigation of electronic properties and polarization effects.[31]

II. METHOD

Density functional theory (DFT)-based Car−Parrinello (CP) MD simulations[32] have been performed at constant volume, starting with the experimental density of water at room temperature. The initial system consists of 64 equilibrated water molecules in a supercell with body-centered-cubic symmetry[33] and periodic boundary conditions. Subsequently, two adjacent water molecules have been replaced by a methane molecule, the resulting solution system being characterized by a density of 0.98 g/cm^3, in line with the typical density considered in previous simulations.[3,31,34] Then, the novel system has been reequilibrated for 2 ps to allow water molecules to reorganize and form the solvation shell around the solute. Then, statistics have been collected for about 20 ps, while the temperature of the system has been controlled by a Nosé−Hoover chain thermostat[35] on the ionic degrees of freedom. For comparison with the properties of pure water, a parallel simulation with a system of 64 water molecules at the same conditions has been performed. In line with the approach followed in recent simulations,[22,36] the chosen target simulation temperatures were higher than the room temperature of actual

dx.doi.org/10.1021/jp300774z | J. Phys. Chem. B 2012, 116, 4552−4560

experiments, since standard DFT functionals (such as the PBE adopted here) are known to be affected by a slight overbinding, leading to a sort of "glassy behavior" of the dynamics around room temperature,[21,37] which is probably partially related to the neglect of proton quantum effects[20] and to the well-known deficiencies of standard DFT approaches in describing van der Waals interactions;[38] note that the lack of an accurate description of the van der Waals interactions in the solvation of small hydrophobic molecules is however expected to have little influence on the surrounding water structure.[1] According to extensive tests[22,37,39] on liquid water simulations with the PBE functional, a 400 K temperature guarantees a liquid-like dynamical behavior of the pure-water system. In order to both directly verify this conclusion and also test its validity for aqueous solution systems, we have performed first principles CP simulations by selecting target average temperatures of 330, 400, and 460 K for pure water and 400 and 460 K for the water−methane solution. H nuclei were treated as classical particles with the mass of deuterium which allows us to use larger time steps,[40] and the effective mass for the fictitious dynamics of the electrons was 700 au with a MD time step of 0.121 fs; such an electronic fictitious mass is within the range suggested (≤370 and ≤760 au for H_2O and D_2O, respectively) to get an accurate description of the electronic ground state and reliable structural and dynamical properties.[20] The number (62) of solvent water molecules is expected to be sufficient, since both experiments[41] and previous simulations[8,15,16,24,42] indicate that solute-induced perturbations are short-ranged. The computations were performed at the Γ-point only of the Brillouin zone, using norm-conserving Troullier−Martins[43] pseudopotentials with a plane-wave cutoff of 80 Ry and the gradient-corrected PBE density functional,[44] which gives[20−22,36] a good description of H bonding in liquid water.

III. RESULTS

A. Structural Properties. Concerning the structural properties, in Figure 1, we show our computed O−O pair correlation function, $g_{OO}(r)$, of pure water at the different temperatures considered in the present simulations, while in Figure 2 we report the $g_{OO}(r)$ and $g_{CO}(r)$ functions of the water−methane solution, at 400 and 460 K, compared to the corresponding functions obtained for the water−methanol

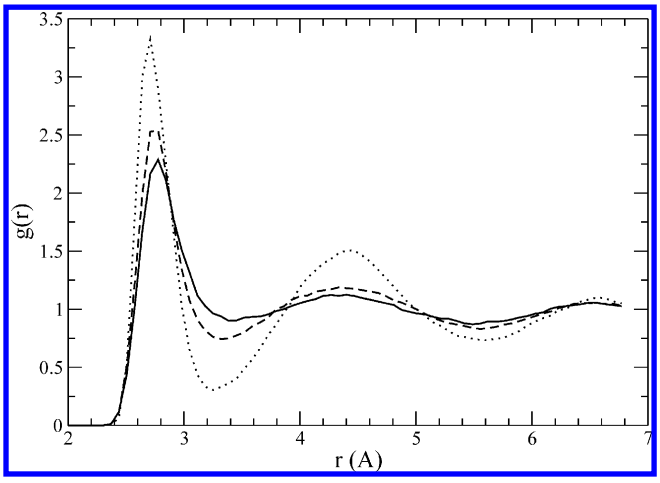

Figure 1. O−O pair-correlation functions of pure water at different simulation temperatures: 330 (dotted line), 400 (dashed line), and 460 K (solid line).

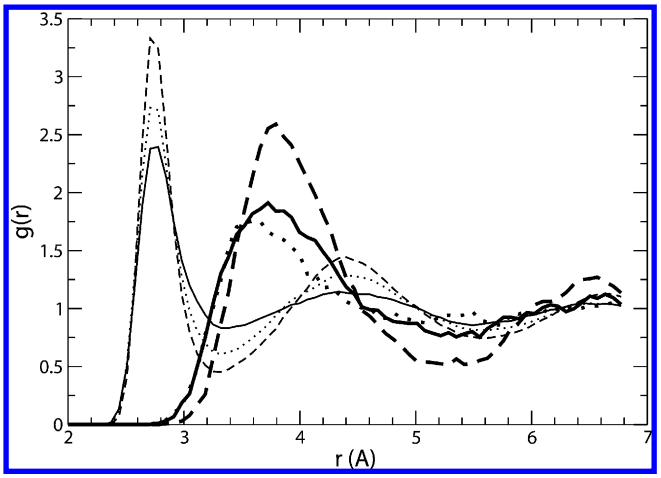

Figure 2. O−O and C−O pair-correlation functions, with the main peak located around 2.8 and 3.5 Å, respectively (the C−O curves are thicker), of water−methane solution at 400 (dashed line) and 460 K (solid line) and of water−methanol at 400 K (dotted line).

solution at 400 K.[17] As expected, the amplitude of the fluctuations of all the pair correlation functions decreases by increasing the temperature; note that our $g_{OO}(r)$ functions computed for pure water (Figure 1) at 400 and 460 K are closer to the experimental[45] $g_{OO}(r)$, obtained at room temperature, than our $g_{OO}(r)$ at 330 K, thus confirming that higher simulation temperatures somehow mimic the missing van der Waals and nuclear effects. Moreover, the $g_{OO}(r)$ functions of the solutions are more structured (Figure 2) than that relative to pure water at the same temperature, in line with the conclusions of previous studies;[3,30,34,46,47] a similar behavior can also be observed for the O−H and H−H pair correlation functions (not shown). The basic structural data (positions and height of the first maximum and first minimum of the pair correlation functions, and coordination number) are listed in Tables 1 and 2, relative to the $g_{OO}(r)$ and $g_{CO}(r)$ functions, respectively. Similarly to the case of aqueous solvation of methanol,[17] the distribution of water O atoms around the C atom of methane is characterized by a broad first peak, located between 3 and 5 Å (see Figure 2), indicating the existence of a solvation shell of about 20 water molecules, in agreement with classical MD simulations.[3,5,31,48] The structure of the methane−water solution in the first hydration shell of methane is determined by a competition between weak methane−water and significantly stronger water−water interactions.[31] A water molecule is defined[34] to be in the hydration shell if its O atom is inside a region around the methane molecule within the first minimum of the $g_{CO}(r)$ function (at about 5.4 Å); bulk molecules are instead those outside the shell. Using the ratio of heights of the first maximum and the following minimum of the $g_{OO}(r)$ pair correlation function as a measure of the degree of structure,[34] looking at Table 1, one can see that it obviously decreases for pure water by increasing the simulation temperature; moreover, with respect to pure water, at 400 K, it is a 2.2 factor larger for the water−methane solution and a 1.3 factor larger for the water−methanol system, and, at 460 K, it is a 1.2 factor larger for the water−methane solution.

The fraction of molecules participating in a given number of Hb's has also been evaluated.[49] Clearly, we focus attention on the water molecules located within the solvation shell, this being a meaningful identification procedure, since the net displacement of both a typical solvent molecule and of the

dx.doi.org/10.1021/jp300774z | J. Phys. Chem. B 2012, 116, 4552−4560

Table 1. First Maximum and First Minimum Height (in Parentheses Position Values in Å) of the O−O Pair Correlation Function, Their Ratio (as a Measure of the Degree of Structure[34]), Nearest Neighbors O−O Distance d_{nn} (in Å), and O−O Coordination Number, n_{OO}[a]

system	first max.	first min.	ratio	d_{nn}	n_{OO}
pure water (330 K)	3.32 (2.71)	0.30 (3.25)	11.1	2.81	4.0
pure water (400 K)	2.54 (2.78)	0.74 (3.32)	3.4	2.80	4.3
pure water (460 K)	2.29 (2.78)	0.90 (3.39)	2.5	2.87	4.7
pure water (298 K, expt.[b])	2.12−2.42 (2.76−2.86)			2.80	
water−methanol (400 K)	2.73 (2.71)	0.61 (3.32)	4.5	2.81	4.2
water−methane (400 K)	3.33 (2.71)	0.45 (3.32)	7.4	2.82	4.2
water−methane (460 K)	2.39 (2.78)	0.83 (3.32)	2.9	2.86	4.3

[a]Water−methanol results are from ref 17. [b]Reference 45.

Table 2. First Maximum and First Minimum Height (in Parentheses Position Values in Å) of the C−O Pair Correlation Function, and C−O Coordination Number, n_{OC}, Compared with Data Obtained by Sequential Quantum Mechanical/Molecular Dynamics Calculations[31] and Monte Carlo Simulations[5]

system	first max.	first min.	n_{OC}
water−methanol (400 K)	1.75 (3.59)	0.86 (5.76)	25.6
water−methane (400 K)	2.59 (3.79)	0.52 (5.28)	19.8
water−methane (460 K)	1.91 (3.72)	0.75 (5.55)	22.2
water−methane (298 K)[a]	1.84 (3.65)	0.82 (5.35)	19.7
water−methane (320 K)[b]	1.43 (3.73)	0.75 (5.4)	17.3

[a]Reference 31. [b]Reference 5.

solute during the simulation is relatively small. In line with previous findings,[8] the water molecules near the apolar methane molecule turn out to have essentially the same average number of Hb's as do the others (see Table 5); since the average distances and angles relative to these Hb's are very similar to those in the bulk, one infers that even the Hb strength is not significantly different. Looking at Table 1, one can see that the nearest neighbor O−O distance is essentially the same in pure water and in the solutions, if comparison is made at the same simulation temperature. This confirms the results of neutron scattering studies which suggest that hydrophobic solutes have surprising little effect on the O−O distances,[50,51] so that it appears that water molecules can change their Hb dynamics and partially lose their reorientation ability without strongly disrupting the local structure.[16,52] The small changes in the structure of the solvating water shell around methane and methanol indicate that the Hb water network is very flexible and can easily accommodate small apolar solute groups without significantly changing its structure, in agreement with previous studies.[3,24,25] The low aqueous solubility of methane makes experimental studies of this system difficult: estimates of the OC coordination number, n_{OC} = 16 and 19, have been calculated from the methane carbon−water oxygen pair correlation function determined from neutron diffraction. Results from computer simulations[3,5,34,48,52] indicate that n_{OC} is in the range 16−22. The chemical shifts in NMR spectra of aqueous methane can be used to measure the number of water molecules in the first hydration sphere of methane because the chemical shift is a measure of the size of the hydrophobic cage around methane: in such a way, it was found that n_{OC} = 20,[48] in good agreement with our findings.

The orientations of the water molecules relative to the methane molecule can be analyzed by computing the angle α subtended by the vector joining the C atom of methane to the O of a water molecule with the vector between the O and a H atom of the water molecule (see Figure 3, showing a typical

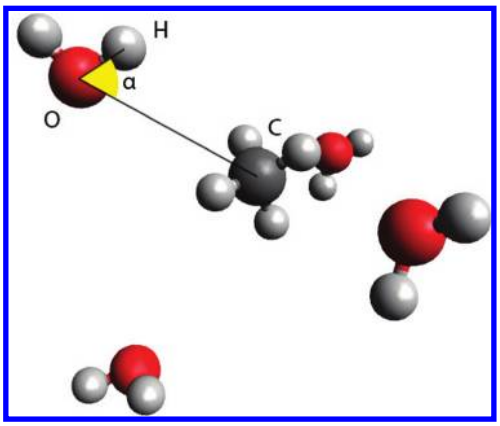

Figure 3. Typical configuration for the four water molecules closest to methane.

configuration for the four water molecules closest to methane). For the water−methane solution, both at 400 and 460 K, we find $\alpha \simeq 91°$ for the water molecules within the solvation shell of methane, which corresponds to an essential tangential orientation of water molecules with respect to the solute's surface. This type of arrangement agrees with previous classical MD estimates[5,53] and allows water molecules to straddle the surface of the solute and maintain a nearly tetrahedral Hb coordination as found in bulk water.

B. Dynamical Properties. More relevant to the comparison with recent experiments is the analysis of the dynamical properties. Our estimated diffusion coefficients (computed by mean-square displacement and relative to the O atoms of the water molecules) in pure water and aqueous solutions are reported in Table 3. As can be seen, in pure water, the diffusion coefficient, D, at the simulation temperature of 400 K is close to the experimental value[54] of bulk liquid heavy water at room temperature, thus confirming that this simulation temperature is adequate to reproduce effective room-temperature conditions (at the simulation temperature of 330 K, D is instead much smaller than the reference value). For the water−methanol solution at 400 K, D is only moderately smaller than in pure water, in agreement with previous simulations[8] that predicted a slower translational diffusion of water in solution. However, for the water−methane system, at 400 K, D is much smaller than the corresponding value of pure water at the same temperature and is close to D of pure water at 330 K, thus suggesting that this strong water mobility reduction is probably not a genuine

dx.doi.org/10.1021/jp300774z | J. Phys. Chem. B 2012, 116, 4552−4560

Table 3. Diffusion Coefficient, D in 10^{-5} cm^2/s (in Parentheses, in the Case of the Solutions, the Reduction Factor with Respect to D of Pure Water at the Same Simulation Temperature)

system	D
pure water (330 K)	0.40
pure water (400 K)	2.60
pure water (460 K)	5.17
pure water (309 K, expt.[a])	1.9
water−methanol (400 K)	1.66 (1.57)
water−methane (400 K)	0.34 (7.65)
water−methane (460 K)	4.29 (1.21)

[a]Reference 54.

physical effect but instead a consequence of the artificial "glassy behavior" of the dynamics discussed above. At 460 K, the D value of water−methane exhibits instead only a moderate reduction with respect to pure water at the same temperature, similarly to the case of water−methanol at 400 K and in line with the results of previous classical MD simulations.[3] These observations suggest that the simulation temperature of 460 K is more suitable for a proper comparison between the properties of the water−methane solution and those of pure water. In principle, we cannot rule out that the glassy behavior observed at 400 K in the water−methane solution could also be related to the relatively small simulation cell we adopted, although it was not observed in our previous simulation of methanol in water,[17] in which the same supercell was used. In order to definitely clarify this point, further (expensive) first principles simulations of water−methane using a supercell of increasing size would be required.

Among the available dynamical observables, the molecule rotational correlation time represents a particularly useful probe of the hydration shell because of its strong dependence on the local Hb configuration (in bulk water, molecular rotation occurs by a concerted mechanism where Hb's are simultaneously broken and reformed[55]). In particular, the rotational motion can be studied by looking at the orientational correlation functions, given by

$$C_l(t) = \langle P_l[\mathbf{u}(t)\mathbf{u}(0)]\rangle \quad (1)$$

where $P_l(x)$ is the Legendre polynomial of order l and $\mathbf{u}$ is a unit vector along the molecular dipole moment or the HOH angle bisector of the water molecules. These orientational correlation functions can be related to experimental measurements and different techniques are sensitive to the first or second order dipole correlation function:[56] DR and Thz time domain spectroscopy probe the decay of $C_1(t)$, while fs-IR (the technique used by Rezus and Bakker[2]), NMR, and optical Kerr-effect spectroscopy probe the decay of $C_2(t)$. By assuming an exponential decay of the $C_1(t)$ and $C_2(t)$ functions, one can easily estimate, by a fitting and/or integration procedure (see, for instance, ref 57), the corresponding reorientation times, τ_1 and τ_2, which are reported in Table 4.

In Figure 4, we plot $C_2(t)$ relative to pure water and water−methane solution at 400 and 460 K (the corresponding figure, relative to water−methanol was already reported and discussed in ref 17). As can be seen, all the functions exhibit an initial rapid decay during the first half ps, which can be attributed[8,56] to overall molecular oscillation (libration) with a loss of phase memory, but without significant net reorientation, keeping the Hb's intact. By considering that the experimental anisotropy

Table 4. Reorientation Times, τ_1 and τ_2 (in Parentheses Divided by the Corresponding Quantities of Pure Water at the Same Temperature), and τ_1/τ_2 Ratio, of All the Water Molecules, and, for the Solutions, of Bulk Waters, BW, Solvation-Shell Water Molecules, SW, and the Four Waters Closest to Methanol or Methane, 4W (see Figure 3)[a]

system	τ_1 (ps)	τ_2 (ps)	τ_1/τ_2
pure water (330 K)	15.8	5.9	2.7
pure water (400 K)	3.4	1.4	2.5
pure water (460 K)	1.5	0.6	2.6
pure water (300 K, classical MD[b])	4.3	2.0	2.1
pure water (283 K, classical MD[c])	3.3	1.1	2.9
pure water (300 K, expt.[b])	2−7.5	1.7−2.6	
water−methanol (400 K)	3.8 (1.1)	1.8 (1.3)	2.1
water−methanol (400 K) BW	4.1 (1.2)	1.9 (1.3)	2.2
water−methanol (400 K) SW	4.3 (1.3)	2.0 (1.4)	2.2
water−methanol (400 K) 4W	5.2 (1.5)	2.2 (1.6)	2.4
water−methane (400 K)	10.6 (3.1)	4.9 (3.6)	2.1
water−methane (400 K) BW	14.0 (4.1)	5.8 (4.2)	2.4
water−methane (400 K) SW	9.1 (2.6)	4.4 (3.2)	2.1
water−methane (400 K) 4W	22.6 (6.6)	8.6 (6.2)	2.6
water−methane (460 K)	1.9 (1.3)	0.7 (1.3)	2.6
water−methane (460 K) BW	1.9 (1.3)	0.8 (1.4)	2.4
water−methane (460 K) SW	2.3 (1.5)	0.7 (1.3)	3.3
water−methane (460 K) 4W	2.4 (1.6)	0.9 (1.6)	2.7
water−TMAO (298 K, classical MD[d])		2.8−3.4 (1.3−1.5)	

[a]Classical MD results of ref 9 have been obtained by simulations of an aqueous solution, at 0.1 molality, of trimethylamine-*N*-oxide (TMAO), representative of a typical hydrophobic solute. [b]Reference 10. [c]Reference 3. [d]Reference 9.

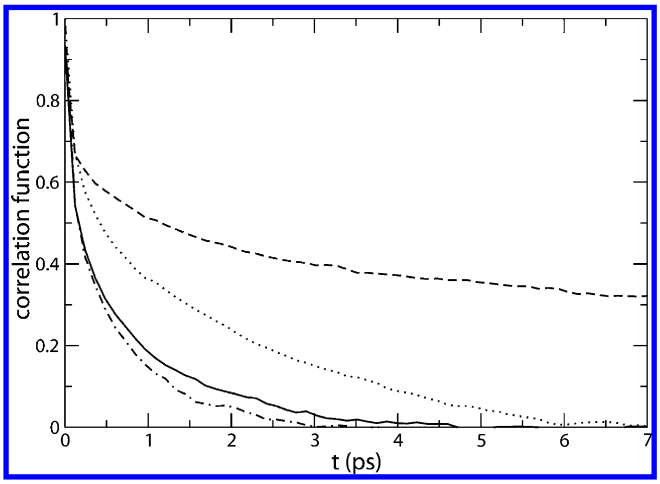

Figure 4. $C_2(t)$ function in the water−methane solution at 400 (dashed line) and 460 K (solid line) and in pure water at 400 (dotted line) and 460 K (dot-dashed line).

function is given by $2/5C_2(t)$,[9] our computed $C_2(t)$ curve, at 460 K, resembles the time-dependent anisotropy measured, at low concentration, with pump−probe spectroscopy (see, for instance, Figure 1 of ref 9 and Figure 3 of ref 16). In qualitative agreement with previous classical MD simulations,[3] the decay of $C_2(t)$, at 460 K, is found to be not much slower in solution than in pure water, without any noticeable plateau; instead, at

dx.doi.org/10.1021/jp300774z | J. Phys. Chem. B 2012, 116, 4552−4560

400 K, the decay of our computed $C_2(t)$ turns out to be much slower in the water−methane solution than in bulk water.

The reorientation times (see Table 4), estimated from the analysis of the $C_2(t)$ functions, relative to all the water molecules, and, for the solutions, also to bulk waters, solvation-shell water molecules, and the four waters closest to methanol or methane (roughly corresponding to integration of the $g_{CO}(r)$ pair correlation function up to the position of the first maximum), are only slightly longer than that in pure water if comparison is done between water−methanol and pure water at 400 K and between water−methane and pure water at 460 K. In line with the behavior of the diffusion coefficient discussed above and with the slow decay of the $C_2(t)$ function shown in Figure 4, the reorientation times of the water−methane solution at 400 K appear to be instead much larger than in pure water, thus strengthening the conclusion that the system is characterized by an artificial "glassy behavior" at that simulation temperature. At the temperature of 460 K, comparison with pure water properties indicates a much more reasonable behavior, thus indicating that the proper effective simulation temperature to be used to reproduce ambient condition properties is not necessarily the same for pure water and for solutions or confined water. As can be seen in Table 4, in the solutions, there is no significant difference between the retardation of the rotational motion of bulk waters and solvation waters; only the four waters closest to methanol or methane appear to undergo a little more pronounced slowing-down effect. Our predicted moderate slowing down of water molecules around methane and methanol is in good agreement with the results of classical MD simulations,[3,9,30] although the absolute values of our estimated reorientation times are significantly shorter than those (2.8−4.5 ps) obtained by some simulations[9,30] and in better agreement with the data reported by Laaksonen and Stilbs[3] and with experimental estimates (1.7−2.6 ps in pure water[58]), thus confirming that reorientation rates are often overestimated in classical MD simulations.[8] Concerning the τ_1/τ_2 ratio, its value smaller than 3 indicates that the reorientation motion of water molecules, both in bulk and in solutions, cannot be entirely ascribed to a pure diffusive mechanism, which would lead to a value of 3.[10]

C. Hydrogen Bond Structure and Dynamics. In Table 5, we report the basic data about the Hb structure. As can be seen, the average number of Hb's per water molecule, N_{Hb}, slightly increases in solutions compared to the value of pure water at the same simulation temperature. Moreover, as already pointed out above, the average number of Hb's for the four water molecules closest to the methane molecule does not much differ from (and in any case is not smaller than) that of the other waters. Therefore, we can conclude that, as already suggested elsewhere,[34] the enhanced structure of the O−O pair correlation functions mainly reflects the fact that water is excluded from the region occupied by the solute molecule and does not indicate a pronounced increase in water−water structure. The fraction of broken Hb's can be defined[5] as $f = (4 - N_{Hb})/2$, where N_{Hb} is the average number of Hb's per water molecule. We find that, at 400 K, f = 0.26, 0.22, and 0.11 for pure water, water−methanol, and water−methane, respectively, while, at 460 K, f = 0.35 and 0.28 for pure water and water−methane, respectively, thus confirming again that small solutes like methanol and methane not only do not disrupt the Hb structure of bulk water, but they even show a tendency to enhance it, since the fraction of broken Hb's is slightly reduced in the aqueous solutions.

Table 5. Average Number of Hb's per Water Molecule, N_{Hb}, Average Lifetime of Water−Water Hb's of All the Water Molecules, τ_{Hb}, and, for the Solutions, of the Four Waters Closest to Methanol or Methane, 4W (in Parentheses Divided by the Corresponding Quantities of Pure Water at the Same Temperature)

system	N_{Hb}	τ_{Hb} (ps)
pure water (330 K)	3.79	2.37
pure water (400 K)	3.51	0.76
pure water (460 K)	3.33	0.47
pure water (300 K, classical MD[a])	3.34−3.78	0.68−1.03
water−methanol (400 K)	3.56 (1.02)	1.01 (1.33)
water−methanol (400 K) 4W	3.56	0.99 (1.30)
water−methane (400 K)	3.71 (1.09)	1.70 (2.24)
water−methane (400 K) 4W	3.80	1.86 (2.45)
water−methane (460 K)	3.38 (1.04)	0.62 (1.32)
water−methane (460 K) 4W	3.40	0.69 (1.47)
water−methane (320 K, classical MD[b])	3.52	

[a]Reference 64. [b]Reference 5.

In bulk liquid water, the reorientation of water molecules involves large angular jumps and proceeds through a concerted mechanism in which a rotating water molecule breaks a Hb with an overcoordinated first neighbor, while forming a new bond with an undercoordinated molecule initially located on the inner side of the second solvation shell (with typical energy barriers of the order of 4 kcal/mol).[37] Experiments and simulations for pure water have led to a detailed picture of water motion at very short times (less than 100 fs), followed by rotational jumps and Hb making and breaking at longer times (of the order of 1−2 ps): the Hb exchange mechanism occurs by means of large (about 60°), very fast (about 200 fs) but relatively seldom (once in 2−3 ps) angular jumps corresponding to concerted Hb switching events.[10,16,55,57,59,60]

In Table 5, we also list the average Hb lifetimes, estimated by considering the persistence of all the Hb atom pairs during the MD trajectory. As can be seen, the average Hb lifetimes of the four water molecules closest to the methane are slightly longer (by about a 1.1 factor) than the value of all the waters. Interestingly, the situation is different for aqueous solvation of methanol, which is characterized by the presence of a hydrophilic group too: in fact, the average Hb lifetime of the four water molecules closest to the CH_3 group of methanol is marginally shorter that that of all the water molecules. The longer average Hb lifetimes at the interface relative to the interior can be attributed to the lack of cooperative effects in proximity to methane due to the decreased density of water.[61] In fact, by considering the mechanism of Hb exchange,[57] in order to undergo Hb exchange, a water molecule must have a readily available Hb partner in the second hydration shell; at the interface, the number of nearest neighbor water molecules decreases; this reduces the probability of there being a nearby water molecule that may accept a newly formed Hb and thus lengthens the lifetime of already formed Hb's. Note that the rotational dynamics of water are inherently connected to the Hb dynamics, since for the rotational correlation to decay to zero the water−water Hb network must lose all correlation with its former state. These reorientation times therefore are expected to be roughly proportional to the Hb lifetimes,[57] since the Hb exchange has been shown to be the main water reorientation pathway.[9−11] This expectation is confirmed by our data if one compares the τ_2 values of Table 4 to the τ_{Hb}

dx.doi.org/10.1021/jp300774z | J. Phys. Chem. B 2012, 116, 4552−4560

estimates of Table 5. Clearly, the presence of a hydrophobic group blocks the approach of some new water Hb acceptors, thus retarding the jump rate between Hb acceptors for surrounding waters, as observed in previous, classical MD simulations.[9] The jump time increase with increasing solute concentration can be quantitatively described by a transition state excluded-volume model:[9] the slowdown factor (or retardation factor) with respect to the bulk is $\rho_v = 1/(1 - f)$, where f is the fraction of transition state locations for the new acceptor which are forbidden by the solutes's presence.[9,15]

In the case of solvation of methane, a methane molecule excludes the centers of water molecules from a spherical volume less than 5 Å across; this volume is small enough that its presence in water requires no breaking of Hb's: water molecules can adopt orientations that allow the Hb pattern to go around the solute, and the extent to which bonds are broken at any instant is similar to that in the pure liquid.[1] In the case of water−methane at 460 K, by estimating the excluded volume fraction and the consequent retardation factor,[9] we obtain 0.26 and 1.35, in good agreement with the predictions (0.28 and 1.39, respectively) of Laage et al.[9] Note that this retardation factor matches well with the slowing-down factor (1.3) derived by the reorientation time analysis, thus indicating that the rotational slowing down is compatible with the one predicted on the basis of the excluded volume fraction. As discussed above, compared to pure water, the water structure is slightly enhanced in the presence of methane. Of course, the enhanced water structure in the first hydration shell implies longer lifetimes for the Hb's and, evidently, hindered dynamics: the effect is equivalent as lowering the temperature in the vicinity of the solute,[3] which could also partially explain the "glassy behavior" of the water−methane solution at 400 K.

D. Electronic (Polarization) Properties. In contrast to simulations based on semiempirical potentials, first principles schemes yield detailed information also on the electronic charge distributions, which in liquid and aqueous solvation systems can be conveniently elaborated using the maximally localized Wannier function (MLWF) method.[19,25,26,62] In condensed phases, the self-consistent internal electric field polarizes the water and solute molecules, leading to a large increase of their molecular dipole moments. Using the MLWF scheme,[19,26,62] the dipole moment of a system can be simply calculated by assuming that the electronic charge is concentrated in point charges located at the positions of the Wannier function centers.

Our computed dipole moments are reported in Table 6. In bulk liquid water, the average value of the dipole moment per water molecule is enhanced by about 80%, with respect to that of the isolated water monomer (1.88 D, experimental: 1.86 D), this being a typical feature of strongly Hb molecules. However, as can be seen, the presence of the solutes affects the distribution of the water-molecule dipole moments: in fact, considering the associated statistical errors, the average dipole moments of water molecules in the solvation shells are significantly smaller than those of the bulk waters (the effect is more pronounced for methanol, which is understandable, since this molecule is also characterized by the presence of a hydrophilic termination). This suggests that the presence of the solute reduces the polarization effects in the solvation-shell waters, which is compatible with the fact that the rotational mobility is not much decreased: in fact, one expects that a smaller dipole moment makes the reorientation of water molecules easier, in such a way to partially offset the increased

Table 6. Average Dipole Moment, μ, of the Bulk Water Molecules, BW, and, for the Solutions, of the Solvation Shell Waters, SW, the Four Waters Closest to Methanol or Methane, 4W, and of Methanol or Methane

system	μ (D)
pure water (400 K)	3.49 ± 0.16
pure water (460 K)	2.94 ± 0.01
water−methanol (400 K) BW	3.56 ± 0.17
water−methanol (400 K) SW	3.05 ± 0.02
water−methanol (400 K) 4W	3.02 ± 0.04
water−methanol (400 K) methanol	3.05 ± 0.10
water−methane (400 K) BW	3.16 ± 0.02
water−methane (400 K) SW	3.05 ± 0.02
water−methane (400 K) 4W	3.00 ± 0.06
water−methane (400 K) methane	0.26 ± 0.03
water−methane (460 K) BW	2.99 ± 0.02
water−methane (460 K) SW	2.94 ± 0.02
water−methane (460 K) 4W	2.93 ± 0.04
water−methane (460 K) methane	0.34 ± 0.04

tendency to rigidity of waters in the solvation shell (water rotation is very fast in the limiting case of water dispersed in an apolar solvent[63]). Clearly, such an effect cannot be reproduced by most of the classical MD simulations where nonpolarizable models for the water molecules (which are often assumed to be rigid and equal) are adopted and could explain why the ratio between our estimated reorientation times of waters in solution and in pure water is smaller than that (1.5−2.0) obtained by classical MD methods based on rigid force field and instead closer to that (1.3) given by flexible-force field simulations.[8,9]

Recently, Mateus et al.[31] have investigated the electronic properties of a methane−water solution by a sequential quantum mechanical/MD approach and found that, upon hydration, methane acquires an induced dipole moment of 0.48 ± 0.20 D, due to polarization effects and to weak methane−water Hb interactions, a value comparable to our estimates in Table 6. Mateus et al.[31] found no difference between the average monomeric dipole moment of bulk waters and that of waters in close interaction (within the first hydration layer of) with methane; instead, we find a slight reduction. This difference is probably due to the fact that in the simulations of Mateus et al. the geometry of the water molecules was kept rigid while only that of methane was flexible, at variance with our approach.

IV. CONCLUSIONS

In conclusion, our results, compatible with recent experiments, shed light on the controversial issue related to the presence of "immobilized" water molecules around hydrophobic groups. Since there is no evidence that a few waters rotate much more slowly than the others in solution, one concludes that the presence of the hydrophobic solute slightly reduces the mobility of many water molecules, rather than immobilizing just the few ones which are closest to the methane molecule, similarly to what was obtained by simulations of soluted methanol, and in line with the interpretation of Qvist and Halle[12] and with classical MD simulation results.[9,30] Therefore, our results are also relevant to validate the classical MD approach for modeling of aqueous solutions. Moreover, the rotational slowing down is compatible with the one predicted on the basis of the excluded volume fraction, which leads to a slower hydrogen bond exchange rate. By generating maximally

dx.doi.org/10.1021/jp300774z | J. Phys. Chem. B 2012, 116, 4552−4560

localized Wannier functions, a detailed description of the polarization effects in both solute and solvent molecules has been obtained, which better characterizes the solvation process. Finally, the analysis of simulations performed at different temperatures suggests that the target temperature of the soluted system must be carefully chosen, in order to avoid artificial slowing-down effects.

AUTHOR INFORMATION

Notes

The authors declare no competing financial interest.

ACKNOWLEDGMENTS

Allocation of computer resources from INFM "Progetto Calcolo Parallelo" is acknowledged.

REFERENCES

(1) Chandler, D. *Nature* **2005**, *437*, 640−647. Pal, S. K.; Zewail, A. H *Chem. Rev.* **2004**, *104*, 2099−2124.
(2) Rezus, Y. L. A.; Bakker, H. J. *Phys. Rev. Lett.* **2007**, *99*, 148301.
(3) Laaksonen, A.; Stilbs, P. *Mol. Phys.* **1991**, *74*, 747−764.
(4) Chandler, D. *Nature* **2002**, *417*, 491.
(5) Chau, P. L.; Mancera, R. L. *Mol. Phys.* **1999**, *96*, 109−122.
(6) Lambeth, B. P.; Junghans, C.; Kremer, K; Clementi, C.; Delle Site, L. *J. Chem. Phys.* **2010**, *133*, 221101.
(7) Frank, H. S.; Evans, M. W. *J. Chem. Phys.* **1945**, *13*, 507−532. Franks, F.; Ives, D. J. *Rev. Chem. Soc.* **1966**, *20*, 1−44. Ludwig, R. *Chem. Phys.* **1995**, *195*, 329−337. Lamanna, R.; Cannistraro, S. *Chem. Phys.* **1996**, *213*, 95−110.
(8) Rossky, P. J.; Karplus, M. *J. Am. Chem. Soc.* **1979**, *101*, 1913−1937. Zichi, A. D.; Rossky, P. J. *J. Chem. Phys.* **1986**, *84*, 2814−2822. Turner, J.; Soper, A. K. *J. Chem. Phys.* **1994**, *101*, 6116−6125. Sidhu, K. S.; Godfellow, J. M.; Turner, J. Z. *J. Chem. Phys.* **1999**, *110*, 7943−7950. Fidler, J.; Rodger, P. M. *J. Phys. Chem. B* **1999**, *103*, 7695−7703.
(9) Laage, D.; Stirnemann, G.; Hynes, J. T. *J. Phys. Chem. B* **2009**, *113*, 2428−2435. Laage, D. *J. Phys. Chem. B* **2009**, *113*, 2684−2687.
(10) Laage, D.; Hynes, J. T. *Science* **2006**, *311*, 832−835.
(11) Sciortino, F.; Geiger, A.; Stanley, H. E. *Nature* **1991**, *354*, 218−221. Gallagher, K. R.; Sharp, K. A. *J. Am. Chem. Soc.* **2003**, *125*, 9853−9860.
(12) Qvist, J.; Halle, B. *J. Am. Chem. Soc.* **2008**, *130*, 10345−10353.
(13) Yoshida, K.; Ibuki, K.; Ueno, M. *J. Chem. Phys.* **1998**, *108*, 1360−1367. Haselmaier, R.; Holz, M.; Marbach, W.; Weingartner, H. *J. Phys. Chem.* **1995**, *99*, 2243−2246. Shimizu, A.; Fumino, K.; Yukiyasu, K.; Taniguchi, Y. *J. Mol. Liq.* **2000**, *85*, 269−278. Okuchi, S.; Moto, T.; Ishihara, Y.; Numajiri, H.; Uedaira, H. *J. Chem. Soc., Faraday Trans.* **1996**, *92*, 1853−1857. Ishihara, Y.; Okouchi, S.; Uedaira, H. *J. Chem. Soc., Faraday Trans.* **1997**, *93*, 3337−3342. Kaatze, U.; Gerke, H.; Pottel, R. *J. Phys. Chem.* **1986**, *90*, 5464−5469. Wachter, W.; Buchner, R.; Hefter, G. *J. Phys. Chem. B* **2006**, *110*, 5147−5154.
(14) Fecko, C. J.; Eaves, J. D.; Loparo, J. J.; Tokmakoff, A.; Geissler, P. L. *Science* **2003**, *301*, 1698−1702.
(15) Stirnemann, G.; Hynes, J. T.; Laage, D. *J. Phys. Chem. B* **2010**, *114*, 3052−3059.
(16) Bakulin, A. A.; Liang, C.; la Cour Jansen, T.; Wiersma, D. A.; Bakker, H. J.; Pshenichnikov, M. S. *Acc. Chem. Res.* **2009**, *113*, 1229−1238. Bakulin, A. A.; Pshenichnikov, M. S.; Bakker, H. J.; Petersen, C. *J. Phys. Chem. A* **2011**, *115*, 1821−1829.
(17) Silvestrelli, P. L. *J. Phys. Chem. B* **2009**, *113*, 10728−10731.
(18) Sprik, M.; Hutter, J.; Parrinello, M. *J. Chem. Phys.* **1996**, *105*, 1142−1152.
(19) Silvestrelli, P. L.; Parrinello, M. *Phys. Rev. Lett.* **1999**, *82*, 3308−3311. Silvestrelli, P. L.; Parrinello, M. *J. Chem. Phys.* **1999**, *111*, 3572−3580.
(20) Grossman, J. C.; Schwegler, E.; Draeger, E. W.; Gygi, F.; Galli, G. *J. Chem. Phys.* **2004**, *120*, 300−311. Schwegler, E.; Grossman, J. C.; Gygi, F.; Galli, G. *J. Chem. Phys.* **2004**, *121*, 5400−5409.
(21) VandeVondele, J.; Mohamed, F.; Krack, M.; Hutter, J.; Sprik, M.; Parrinello, M. *J. Chem. Phys.* **2005**, *122*, 014515.
(22) Sit, P. H.-L.; Marzari, N. *J. Chem. Phys.* **2005**, *122*, 204510.
(23) Marx, D.; Sprik, M.; Parrinello, M. *Chem. Phys. Lett.* **1997**, *273*, 360−366. Raugei, S.; Klein, M. *J. Chem. Phys.* **2002**, *116*, 196−202.
(24) van Erp, T. S.; Meijer, E. J. *Chem. Phys. Lett.* **2001**, *333*, 290−296.
(25) van Erp, T. S.; Meijer, E. J. *J. Chem. Phys.* **2003**, *118*, 8831−8840.
(26) Scipioni, R.; Schmidt, D. A.; Boero, M. *J. Chem. Phys.* **2009**, *130*, 024502.
(27) Ikeda, T.; Terakura, K. *J. Chem. Phys.* **2003**, *119*, 6784−6788.
(28) Boero, M.; Terakura, K.; Tateno, M. *J. Am. Chem. Soc.* **2002**, *124*, 8949−8957.
(29) Boero, M.; Tateno, M.; Terakura, K.; Oshiyama, A. *J. Chem. Theory Comput.* **2005**, *1*, 925−934.
(30) Ferrario, M.; Haughney, M.; McDonald, I. R.; Klein, M. L. *J. Chem. Phys.* **1990**, *93*, 5156−5166.
(31) Mateus, M. P. S; Galamba, N.; Costa Cabral, B. J.; Coutinho, K.; Canuto, S. *Chem. Phys. Lett.* **2011**, *506*, 183−189.
(32) Car, R.; Parrinello, M. *Phys. Rev. Lett.* **1985**, *55*, 2471−2474. We have used the code CPMD developed by J. Hutter et al., http://www.cpmd.org.
(33) Such a "truncated octahedron" unit cell is often used in simulations of liquids, since it more closely approaches a sphere and is therefore more isotropic.
(34) Bridgeman, C. H.; Buckingham, A. D.; Skipper, N. T. *Chem. Phys. Lett.* **1996**, *253*, 209−215.
(35) Nosé, S. *Mol. Phys.* **1984**, *52*, 255−268. Nosé, S. *J. Chem. Phys.* **1984**, *81*, 511−519. Hoover, W. G. *Phys. Rev. A* **1985**, *31*, 1695−1697.
(36) Sharma, M.; Resta, R.; Car, R. *Phys. Rev. Lett.* **2007**, *98*, 247401.
(37) Paesani, F. *J. Phys. Chem. A* **2011**, *115*, 6861−6871.
(38) Yoo, S.; Xantheas, S. S. *J. Chem. Phys.* **2011**, *134*, 121105.
(39) Yoo, S.; Zeng, X. C.; Xantheas, S. S. *J. Chem. Phys.* **2009**, *130*, 221102.
(40) Laasonen, K.; Sprik, M.; Parrinello, M. *J. Chem. Phys.* **1993**, *99*, 9080−9089. When nuclear motion is treated classically, H_2O and D_2O are expected to yield nearly identical structural properties; of course, the effect is more appreciable concerning dynamical properties, but it is well known: for instance, studies on bulk water (*J. Chem. Phys.* **2004**, *121*, 5992−6002) indicate that relaxation times in D_2O are increased by a factor of about 1.2 with respect to H_2O.
(41) Woessner, D. E. *J. Magn. Reson.* **1980**, *39*, 297−308. Carlström, G.; Halle, B. *Langmuir* **1988**, *4*, 1346−1352.
(42) Vaisman, I. I.; Brown, F. K.; Tropsha, A. *J. Phys. Chem.* **1994**, *98*, 5559−5564. Paschek, D. *J. Chem. Phys.* **2004**, *120*, 10605−10617.
(43) Troullier, N.; Martins, J. L. *Phys. Rev. B* **1991**, *43*, 1993−2006.
(44) Perdew, J. P.; Burke, K.; Ernzerhof, M. *Phys. Rev. Lett.* **1996**, *77*, 3865−3868.
(45) Soper, A. K. *J. Phys.: Condens. Matter* **2007**, *19*, 335206.
(46) Okazaki, S.; Touhara, H.; Nakanishi, K. *J. Chem. Phys.* **1984**, *81*, 890−894.
(47) Jorgensen, W. L.; Madura, J. D. *J. Am. Chem. Soc.* **1983**, *105*, 1407−1413.
(48) Dec, S. F.; Bowler, K. E.; Stadterman, L. L.; Koh, C. A.; Sloan, E. D., Jr. *J. Am. Chem. Soc.* **2006**, *128*, 414−415.
(49) Here, Hb's are identified according to the following geometrical criterion: two molecules are H bonded when the distance between the O atom of one molecule and a H atom of the other is in the range 1.5−2.4 Å and the O−H···O angle is in the range 120−180° (see, for instance, Molteni, C.; Parrinello, M. *J. Am. Chem. Soc.* **1998**, *120*, 2168−2171); the results are not qualitatively changed by adopting other reasonable Hb criteria.
(50) Bezzabotnov, V. Y.; Cser, L.; Grosz, T.; Jancso, G.; Ostanevich, Y. M. *J. Phys. Chem.* **1992**, *96*, 976−982.
(51) Dixit, S.; Crain, J.; Poon, W. C. K.; Finney, J. L.; Soper, A. K. *Nature* **2002**, *416*, 829−832.
(52) Lazaridis, T.; Paulaitis, M. E. *J. Phys. Chem.* **1992**, *96*, 3847−3855.

(53) Tomlinson-Phillips, J.; Davis, J.; Ben-Amotz, D.; Spångberg, D.; Hermansson, K. *J. Phys. Chem. A* **2011**, *115*, 6177−6183.
(54) Lee, H.-S.; Tuckerman, M. E. *J. Chem. Phys.* **2007**, *126*, 164501.
(55) Ramasesha, K.; Roberts, S. T.; Nicodemus, R. A.; Mandal, A.; Tokmakoff, A. *J. Chem. Phys.* **2011**, *135*, 054509.
(56) Tielrooij, K. J.; Petersen, C.; Rezus, Y. L. A.; Bakker, H. J. *Chem. Phys. Lett.* **2009**, *471*, 71−74.
(57) Rosenfeld, D. E.; Schmuttenmaer. *J. Phys. Chem. B* **2011**, *115*, 1021−1031.
(58) Paesani, F.; Voth, G. A. *J. Phys. Chem. B* **2009**, *113*, 5702−5719.
(59) Gaffney, K. J.; Minbiao, J.; Odelius, M.; Sungnam, P.; Sun, Z. *Chem. Phys. Lett.* **2011**, *504*, 1−6.
(60) Skinner, J. L. *Science* **2010**, *328*, 985−986.
(61) Chakraborty, D.; Chandra, A. *Chem. Phys.* **2012**, *392*, 96−104.
(62) Marzari, N.; Vanderbilt, D. *Phys. Rev. B* **1997**, *56*, 12847−12865. Silvestrelli, P. L.; Marzari, N.; Vanderbilt, D.; Parrinello, M. *Solid State Commun.* **1998**, *107*, 7−11.
(63) Goodnough, J. A.; Goodrich, L.; Farrar, T. C. *J. Phys. Chem. A* **2007**, *111*, 6146−6150.
(64) Bergman, D. L. *Chem. Phys.* **2000**, *253*, 267−282.